H_2 Production

DOI: 10.1002/anie.201303110

Exceptional Poly(acrylic acid)-Based Artificial [FeFe]-Hydrogenases for Photocatalytic H_2 Production in Water**

*Feng Wang, Wen-Jing Liang, Jing-Xin Jian, Cheng-Bo Li, Bin Chen, Chen-Ho Tung, and Li-Zhu Wu**

Generation of hydrogen (H_2) from water by solar-energy conversion is considered a promising way to deal with the energy crisis and climate change.[1,2] One of the key challenges at this stage is to create catalysts for H_2 production with high efficiency and low cost. [FeFe]-hydrogenase, an enzyme in algae, is the fastest proton reduction catalyst in nature known to date.[3] The H_2 production rate of the active site of [FeFe]-hydrogenase, a Fe_2S_2 subunit coordinated by CO and CN ligands, achieves turnovers as high as 6000–9000 molecular H_2 per active site per second.[4] Such an efficient catalyst with its noble-metal-free structure has aroused much interest in the last decade.[5,6] With reference to the crystal structure of natural [FeFe]-hydrogenase,[7,8] a large number of [FeFe]-hydrogenase mimics have been synthesized on the basis of the Fe_2S_2 cluster.[9–19] From a photochemical point of view, molecular dyads and triads,[20–25] multi-component systems,[26–33] and assembled hybrid systems,[34–37] have been developed. Although two systems with [FeFe]-hydrogenase mimics as catalysts performed H_2 photo-production with a turnover number (TON) of over 200,[27,28] most of analogous systems finished their photochemical H_2 production with low turnover numbers (TON < 5) in organic solutions or a mixture of organic solvents and water.[12,38,39] In 2011, we designed a robust water-soluble [FeFe]-hydrogenase mimic by linking three hydrophilic ether chains to the Fe_2S_2 active site, and achieved for the first time photocatalytic H_2 production in water.[29] With this water-soluble [FeFe]-hydrogenase mimic as a catalyst, CdTe quantum dots (QDs) as a photosensitizer (PS), and ascorbic acid (H_2A) as a proton source and sacrificial electron donor, the system exhibited a high efficiency for photocatalytic H_2 production (TON = 505). Since then, incorporation of the Fe_2S_2 active site to a water-soluble group,[29,30] protein,[31] and peptide,[32] even the hydrophobic cavity of cyclodextrins,[33] has been developed to realize photocatalytic H_2 production in water because water is believed to be an ideal solvent for proton mobility and has non-toxic as well as economic advantages.[40,41] Indeed, the TON of these water-soluble systems is enhanced in a range of 75 to 84.[30–32] Very recently, a systematic comparison suggested that the efficiency and stability of photocatalytic [FeFe]-hydrogenase systems in water is much better than in organic solvents.[30] Nevertheless, the efficiency for H_2 evolution is far less than the natural [FeFe]-hydrogenase (turnover frequency (TOF) 6000–9000 molecule H_2 per active site per second).

Poly(acrylic acid) (PAA) is a common hydrophilic polymer, widely used in drug-delivery, self-assembly, nanoparticle modification, and bioimaging.[42–45] The carboxy group in the PAA chain not only enhances the water-solubility of the polymer, but also provides modification sites for functionalization. Herein we report that the Fe_2S_2 active site can be anchored on the side chain of water-soluble PAA. With this grafted polymer as a catalyst, CdSe QDs as a photosensitizer, ascorbic acid as proton source and sacrificial electron donor, we have successfully constructed the first set of polymer-based [FeFe]-hydrogenase mimics for photocatalytic H_2 production. The system shows exceptional TON (based on the Fe_2S_2 subunit) and initial TOF of up to 27135 and 3.6 s^{-1}, respectively, for photocatalytic H_2 production in water.

The water-soluble polymer catalyst PAA-*g*-Fe_2S_2 was synthesized by stirring the amine-modified Fe_2S_2 precursor Fe_2S_2-NH_2, which is a deprotected product of Fe_2S_2-NHBoc, in a mixed solution of CF_3COOH and CH_2Cl_2 (v/v = 1/2), and PAA (M_w = 1800) in the presence of PyBOP ((benzotriazol-1-yloxy)tripyrrolidinophosphonium hexafluorophosphate) in a Et_3N/DMF mixed solution at room temperature (Scheme 1).[42,43] The crude polymer product was precipitated in diethyl ether and dissolved in methanol three times and finally obtained as red to yellow solids depending on the grafting amount of Fe_2S_2 active site. The as-prepared product was characterized by ^1H NMR, IR, UV/Vis spectroscopy and GPC (Supporting Information, Figure S1). The ^1H NMR spectra of PAA-*g*-Fe_2S_2 polymer and PAA in D_2O are shown in Figure 1. The signals at δ = 7.56–7.36 ppm (H_a) and δ = 4.33 ppm (H_b) of the PAA-*g*-Fe_2S_2 polymer are attributed to the aromatic protons and methylene protons next to amide of the Fe_2S_2 moiety, respectively. The IR spectrum of PAA-*g*-Fe_2S_2 exhibits a signal for cyanide (CN) at 2125 cm^{-1} and three characteristic CO signals at 2040, 1998, and 1975 cm^{-1} of the Fe_2S_2 active site, which are the same as those in the precursor Fe_2S_2-NHBoc (Figure 2b).[22] The UV/Vis absorption spectra of PAA-*g*-Fe_2S_2 shows a strong characteristic absorption of Fe_2S_2 moiety at 309 nm in water (Figure 2a), which is a blue-shift of 5 nm compared to the

[*] F. Wang, W.-J. Liang, J.-X. Jian, C.-B. Li, Dr. B. Chen, Prof. Dr. C.-H. Tung, Prof. Dr. L.-Z. Wu
Key Laboratory of Photochemical Conversion and Optoelectronic Materials, Technical Institute of Physics and Chemistry & University of Chinese Academy of Sciences, the Chinese Academy of Sciences
Beijing 100190 (P.R. China)
E-mail: lzwu@mail.ipc.ac.cn

[**] We are grateful for financial support from the Ministry of Science and Technology of China (2009CB220008, 2013CB834505 and 2013CB834804), the National Science Foundation of China (21090343, 50973125 and 91027041), and the Knowledge Innovation Program of the Chinese Academy of Sciences.

Supporting information for this article is available on the WWW under http://dx.doi.org/10.1002/anie.201303110.

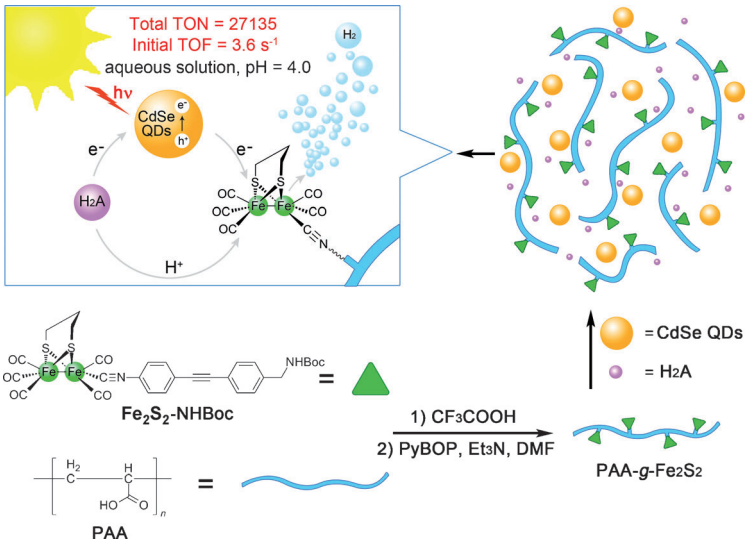

Scheme 1. The synthetic route to PAA-*g*-Fe_2S_2 for the photocatalytic H_2 production.

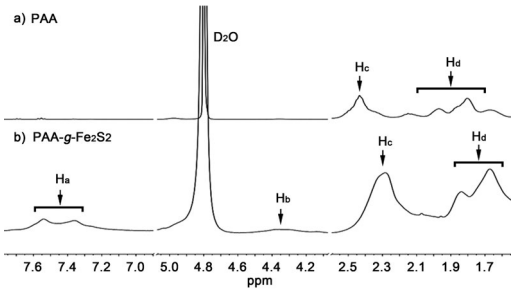

Figure 1. The ^{1}H NMR spectra of a) PAA and b) PAA-*g*-Fe_2S_2 in D_2O.

absorption at 314 nm of precursor Fe_2S_2-NHBoc in CH_3CN. All of these results confirmed the Fe_2S_2 moiety was chemically grafted on the PAA chain.

Using different initial amount of precursor Fe_2S_2-NHBoc, three PAA-*g*-Fe_2S_2 polymer catalysts (PAA-*g*-Fe_2S_2-1, PAA-*g*-Fe_2S_2-2 and PAA-*g*-Fe_2S_2-3) with different amounts of grafted Fe_2S_2 active site were prepared. All three polymer catalysts are quite soluble in water. The grafting amount of Fe_2S_2 active site for PAA-*g*-Fe_2S_2-1, PAA-*g*-Fe_2S_2-2,and PAA-*g*-Fe_2S_2-3 is 3.86×10^{-4}, 7.07×10^{-5}, and 4.07×10^{-6} mol g^{-1}, respectively, which was determined by inductively coupled plasma-atomic emission spectrometry (ICP-AES) for the relative amount of iron in samples.

The photocatalytic H_2 production system was constructed by using the PAA-*g*-Fe_2S_2 polymer as a catalyst, 3-mercaptopropionic acid (MPA) stabilized CdSe QDs (MPA-CdSe QDs) as the photosensitizer, and ascorbic acid (H_2A) as the proton source and sacrificial electron donor. The CdSe QDs was selected as the photosensitizer not only for its broad visible-light absorption, aqueous dispersion, and economical advantage over precious metal photosensitizers, but also for its simpler preparation than its counterpart CdTe QDs.

We investigated the H_2 production activity of the system using moderate Fe_2S_2 grafting amount polymer PAA-*g*-Fe_2S_2-2. The system, containing PAA-*g*-Fe_2S_2-2 (0.25 mg mL^{-1}), MPA-CdSe QDs (0.08 mg mL^{-1}), and H_2A (0.01 M) at initial pH 4.0, evolved H_2 immediately with TON of 392 for 3 h of irradiation (blue LED, $\lambda = 450$ nm). The system showed high activity in the first 3 h; further irradiation led to no obvious improvement in the amount of H_2 production. Control experiments demonstrated that the presence of all of the components in the system, catalyst, photosensitizer, H_2A, and light is necessary for photocatalytic H_2 evolution.

The degradation of catalyst and consumption of H_2A influenced the rate of H_2 production greatly. Increasing or decreasing the pH value of the solution to either 5 or 2 resulted in the rate of H_2 evolution dropping dramatically (Figure 3a), consistent with the reported systems using ascorbic acid as a proton source and sacrificial electron donor.[29–31] The H_2 production rate also depends on the concentration of photosensitizer. At fixed concentration of catalyst PAA-*g*-Fe_2S_2-2 and H_2A,

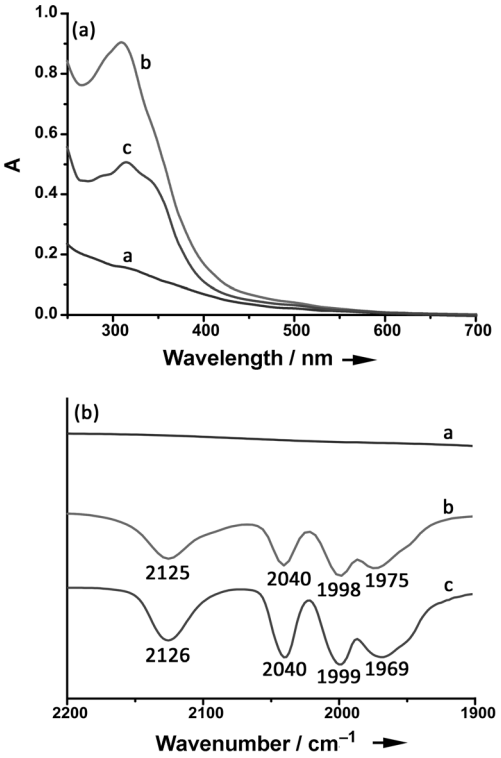

Figure 2. UV/Vis absorption (a) and IR (b) spectra of PAA (line a), PAA-*g*-Fe_2S_2-1 (line b), and Fe_2S_2-NHBoc (Line c); the concentration of samples for UV/Vis absorption is 0.067 mg mL^{-1} for PAA and for PAA-*g*-Fe_2S_2-1 in aqueous solution, and 1.0×10^{-5} M for Fe_2S_2-NHBoc in CH_3CN.

the optimal concentration of photosensitizer was found to be 0.08 mg mL^{-1}, the reaction was accelerated by increasing the concentration of MPA-CdSe QDs from 0.008 mg mL^{-1} to 0.08 mg mL^{-1} in solution (Figure 3b). Further increasing the concentration of CdSe QDs from 0.08 mg mL^{-1} to 0.8 mg mL^{-1}, however, resulted in lower rate of H_2 production and aggregation of CdSe QDs. This change is probably due to

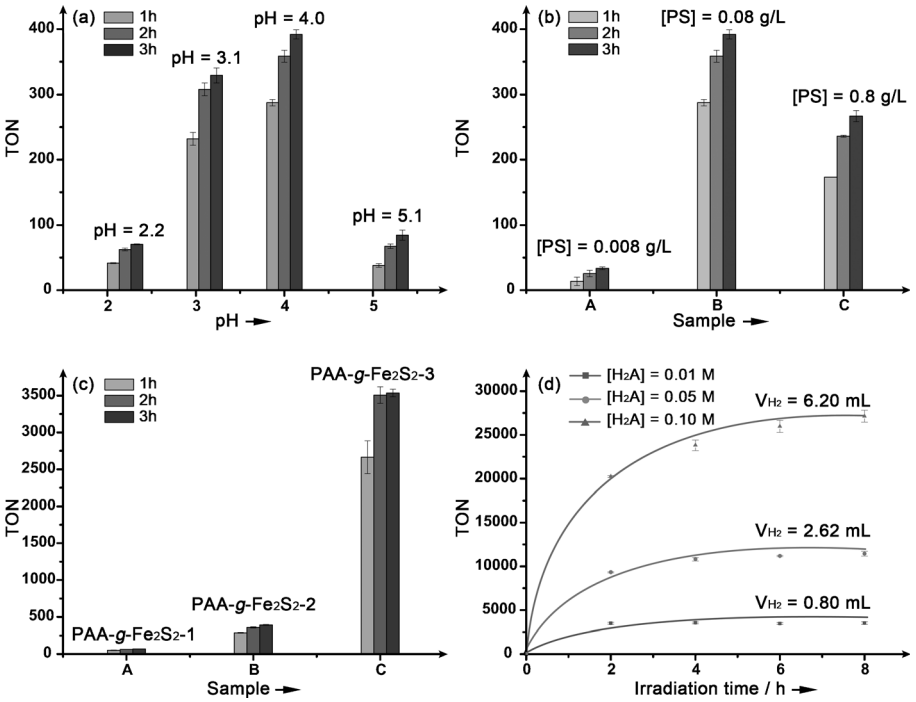

Figure 3. a) Photocatalytic H_2 production in H_2O at different pH values; sample concentration: PAA-*g*-Fe_2S_2-2 (0.25 mg mL^{-1}), MPA-CdSe QDs (0.08 mg mL^{-1}), H_2A (0.01 M); b) Photocatalytic H_2 production at initial pH 4.0 in H_2O as a function of concentration of the photosensitizer (PS) MPA-CdSe QDs; sample concentration: MPA-CdSe QDs (0.008 mg mL^{-1} for sample A, 0.08 mg mL^{-1} for sample B, 0.8 mg mL^{-1} for sample C), PAA-*g*-Fe_2S_2-2 (0.25 mg mL^{-1}), H_2A (0.01 M); c) Photocatalytic H_2 production at initial pH 4.0 in H_2O as a function of catalysts with different loadings of Fe_2S_2 active site; PAA-*g*-Fe_2S_2-1 to PAA-*g*-Fe_2S_2-3 for sample A–C (0.25 mg mL^{-1}), MPA-CdSe QDs (0.08 mg mL^{-1}), H_2A (0.01 M); d) Photocatalytic H_2 production at initial pH 4.0 in H_2O as a function of ascorbic acid concentration; sample concentration: MPA-CdSe QDs (0.08 mg mL^{-1}), PAA-*g*-Fe_2S_2-3 (0.25 mg mL^{-1}), H_2A (0.01 M for line A, 0.05 M for line B, 0.1 M for line C). All samples were irradiated by blue LED lamp ($\lambda = 450$ nm).

the light-filter effect at high concentration of photosensitizer. Next, the H_2 production activity of three PAA-*g*-Fe_2S_2 polymers, PAA-*g*-Fe_2S_2-1, PAA-*g*-Fe_2S_2-2, and PAA-*g*-Fe_2S_2-3, was examined under the identical concentration of photosensitizer and H_2A at pH 4.0. As shown in Figure 3c, PAA-*g*-Fe_2S_2-3, the one with the smallest Fe_2S_2 grafted amount, gives rise to the highest H_2 production efficiency (TON = 3536) of the three PAA-*g*-Fe_2S_2 polymers for 3 h of irradiation. Finally, the photocatalytic H_2 production with the samples containing PAA-*g*-Fe_2S_2-3 (0.25 mg mL^{-1}), MPA-CdSe QDs (0.08 mg mL^{-1}) at different concentrations of H_2A were studied at initial pH 4.0. The rate of photocatalytic H_2 production relies on the concentration of H_2A (Figure 3d), and the initial rate of H_2 production obeys a first-order dependence on the concentration of H_2A (Supporting Information, Figure S2). Surprisingly, the TON reached 27135 for 8 h of irradiation at 0.1 M of H_2A and the rate was as fast as 3.6 molecular H_2 per Fe_2S_2 active site per second in the initial 30 min (Supporting Information). All of these results confirm that the rate of photocatalytic H_2 production depends on pH value of solution, [photosensitizer] ([PS]), [HA^-], and the optical power of light source (Supporting Information, Figure S3). The quantum yield (QY) of the system for H_2 production is 5.07%, which was obtained by the sample of PAA-*g*-Fe_2S_2-1 as catalyst under optimized conditions (Supporting Information). The TON (based on Fe_2S_2 subunit) 27135 and initial TOF 3.6 s^{-1}, to our knowledge, are the highest values reported to date for photocatalytic H_2 production from [FeFe]-hydrogenase mimics.

The photophysical properties of the polymer-based systems were studied to understand the mechanism of the reaction. The average diameter of MPA-CdSe QDs used in our systems is 1.8 nm as determined by TEM. As shown in Figure 4a, the emission spectrum of MPA-CdSe QDs shows a strong excitonic emission at 470 nm and a relative weak and broad surface trap emission ranged from 520–770 nm.[46] With the addition of PAA-*g*-Fe_2S_2-1 or PAA-*g*-Fe_2S_2-2 (1.0 mg) into the aqueous solution of MPA-CdSe QDs (0.08 mg mL^{-1}, 3 mL), the excitonic and trap emissions of CdSe QDs were both quenched. The quenching efficiency estimated at excitonic emission for PAA-*g*-Fe_2S_2-1 and PAA-*g*-Fe_2S_2-2 is 81% and 34%, respectively. Because of the small spectroscopic overlap of absorption of PAA-*g*-Fe_2S_2 and the emission of MPA-CdSe QDs (Supporting Information, Figure S5), the energy transfer between excited MPA-CdSe QDs to PAA-*g*-Fe_2S_2 would be negligible if it occurs, so the emission quenching observed in the cases of PAA-*g*-Fe_2S_2-1 and PAA-*g*-Fe_2S_2-2 is attributed to the photoinduced electron transfer (PET) from the MPA-CdSe QDs to Fe_2S_2 core of PAA-*g*-Fe_2S_2. The rate constant of 6.15×10^{12} M^{-1} s^{-1} for PET was estimated at excitonic emission by the Stern–Volmer equation (Supporting Information, Figure S7). It was worth noting that when the same amount of PAA-*g*-Fe_2S_2-3 or PAA was introduced in the system, the emission intensity of MPA-CdSe QDs increased by 35% or 46%, respectively. The enhancement was also observed by Yang and Gao et al. with the addition of PAA into the aqueous solution of CdTe QDs. They explained and experimentally demonstrated that the coordination between carboxy groups of PAA and cadmium ions on the surface of QDs is responsible for this emission enhancement.[47,48] We believe this coordination works the same way in our case. The PAA chain wraps round the nanoparticles by coordination between the carboxy groups and cadmium ions of CdSe QDs and thus suppresses to some extent the non-radiative decay of MPA-CdSe QDs. Actually, the PAA-*g*-Fe_2S_2 plays two roles for the emission of MPA-CdSe QDs. On the one hand, the Fe_2S_2 active site in PAA-*g*-Fe_2S_2 quenches the emission of MPA-CdSe QDs; on the other hand, the PAA chain suppresses the

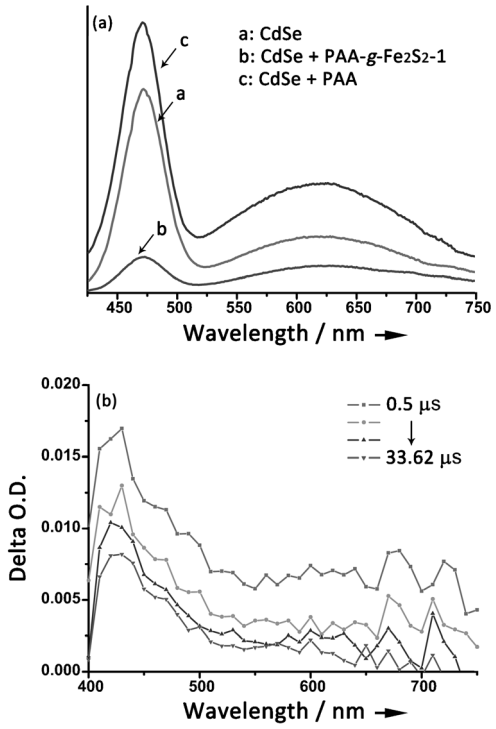

Figure 4. a) The emission spectra of MPA-CdSe QDs (0.08 mg mL^{-1}) in the absence and presence of PAA-*g*-Fe_2S_2-1 (0.33 mg mL^{-1}) or PAA (0.33 mg mL^{-1}) in water; excitation wavelength: 400 nm. b) Transient absorption spectrum of PAA-*g*-Fe_2S_2-1 (1.0 mg mL^{-1}) and MPA-CdSe QDs (0.08 mg mL^{-1}) in H_2O at pH 7.4 upon laser-pulsed by 355 nm light.

mobility of the nanoparticles and enhances the emission of MPA-CdSe QDs. In the cases of PAA-*g*-Fe_2S_2-1 and PAA-*g*-Fe_2S_2-2, the quenching process dominates the overall emission of MPA-CdSe QDs. In contrast, with PAA-*g*-Fe_2S_2-3 the emission of MPA-CdSe QDs is enhanced because of the low amount of Fe_2S_2 active site in PAA-*g*-Fe_2S_2-3.

The electron transfer from excited CdSe QDs to the Fe_2S_2 active site of PAA-*g*-Fe_2S_2 was evidenced by a flash photolysis study at room temperature. Compared with signal silence of a sample of MPA-CdSe QDs with PAA, the solution of CdSe QDs and PAA-*g*-Fe_2S_2-1 at pH 7.4 gave a strong absorption at 430 nm, a broad absorption at the range of 550–650 nm, and a relative strong absorption at 680 nm after excitation by laser light at 355 nm. These absorptions are similar to those reported for Fe^IFe^0 species generated by reduction of [FeFe]-hydrogenase mimics.[20,49] The decay monitored at 430 nm was mono-exponential with a lifetime of 449 µs (Figure S11), which was quenched completely by adjusting the pH to 5.2 by adding HCl to the solution. This quenching is probably due to the formation of protonated $Fe^IFe^{II}H$ species in acidic solution.[39,50–52] The free energy change of electron transfer from excited MPA-CdSe QDs to the Fe_2S_2 core was estimated by the Rehm–Weller equation. The reductive potential ($E_{1/2}$) of −0.43 V (all potentials are versus the normal hydrogen electrode (NHE)) of the Fe_2S_2 active site was taken from cyclic voltammograms obtained using PAA-g-Fe_2S_2-1 in aqueous solution (Figure S12). The valence band energy level (E_{vb}) of CdSe QDs is 0.57 eV,[53] and the excited-state energy (E_{00}) of MPA-CdSe QDs is 2.64 eV. Therefore, the free-energy change (ΔG^0) was determined to be −1.64 eV, indicating that the electron transfer from excited MPA-CdSe QDs to the Fe_2S_2 of PAA-*g*-Fe_2S_2 is exothermic.

From the results described above, we could speculate about the general mechanism of the system. The photoexcited electron in the conduction band of CdSe QDs transfers to the Fe_2S_2 core of PAA-*g*-Fe_2S_2 and generates a one-electron reduced Fe^IFe^0 species. This active species further reacts with a proton in catalytic cycle to produce H_2.[39,50–52] As the oxidative potential of H_2A is negative enough to reduce the CdSe QDs but too positive to reduce the Fe_2S_2 core of PAA-*g*-Fe_2S_2 directly,[54] the oxidative CdSe QDs regenerates by accepting an electron from the sacrificial electron donor HA^-. As reported in the literature and observed in our experiments,[55] the photo-corrosion of CdSe QDs would lead to aggregation of CdSe QDs in aqueous systems. But in this case, the absorption and emission spectra of CdSe QDs (0.08 mg mL^{-1}) were almost unchanged for 4 h of irradiation, and no obvious aggregation was observed in the presence of PAA or PAA-*g*-Fe_2S_2 in aqueous solution (Figures S15 and S16). Evidently, the PAA moiety in PAA-*g*-Fe_2S_2 not only functions as a water-soluble framework to bring the Fe_2S_2 core into water, but also plays a role in protecting MPA-CdSe QDs from photo-corrosion and aggregation. Therefore, it is reasonable to consider that the polymer chain of PAA wraps around the MPA-CdSe QDs by coordination and thus narrows distance between the photosensitizer and the Fe_2S_2 active site in aqueous solution. This unique structure prefers to facilitate electron transfer from the excited MPA-CdSe QDs to PAA-*g*-Fe_2S_2 and consequently improves the rate of photocatalytic H_2 production.

In summary, a new set of water-soluble polymer catalysts PAA-*g*-Fe_2S_2 has been designed and successfully synthesized. A system, containing PAA-*g*-Fe_2S_2 as the catalyst, CdSe QDs as the photosensitizer, and ascorbic acid as proton source and sacrificial electron donor, shows high efficiency for the photocatalytic H_2 production in water. The TON of 27135, initial TOF of 3.6 s^{-1}, are the highest known to date for [FeFe]-hydrogenase mimics, competitive with those from current state-of-the-art catalytic systems for H_2 production. The PAA chain of PAA-*g*-Fe_2S_2 plays three roles in the system: 1) it is a framework to bring the Fe_2S_2 active site into aqueous solution; 2) it is a good stabilizer protecting the MPA-CdSe QDs from aggregation and enhancing the emission quantum yield of the CdSe QDs; 3) it narrows the distance between the photosensitizer and the Fe_2S_2 core for more efficient electron transfer ($k_{ET} = 6.15 \times 10^{12}$ M^{-1} s^{-1}) from the excited MPA-CdSe QDs to the Fe_2S_2 active site. The three functions jointly contribute to a highly efficient photocatalytic H_2 production. Static-state and time-resolved spectroscopic studies demonstrate that the electron transfer from the excited MPA-CdSe QDs to the Fe_2S_2 catalyst center is the key step to trigger the catalytic cycle. The unique performance of the polymer-based [FeFe]-hydrogenase system indicates that this approach is a promising strategy to improve the photocatalytic efficiency of H_2 production in water. Extension of the present systems is ongoing in our laboratory.

Received: April 13, 2013
Published online: June 20, 2013

Keywords: [FeFe]-hydrogenases · hydrogen evolution · photocatalysis · polymers · quantum dots

[1] H. B. Gray, *Nat. Chem.* **2009**, *1*, 7.
[2] A. J. Esswein, D. G. Nocera, *Chem. Rev.* **2007**, *107*, 4022 – 4047.
[3] J. M. Camara, T. B. Rauchfuss, *Nat. Chem.* **2012**, *4*, 26 – 30.
[4] M. Frey, *ChemBioChem* **2002**, *3*, 153 – 160.
[5] J. C. Fontecilla-Camps, A. Volbeda, C. Cavazza, Y. Nicolet, *Chem. Rev.* **2007**, *107*, 4273 – 4303.
[6] M. L. Ghirardi, A. Dubini, J. Yu, P.-C. Maness, *Chem. Soc. Rev.* **2009**, *38*, 52 – 61.
[7] M. W. W. Adams, E. I. Stiefel, *Science* **1998**, *282*, 1842 – 1843.
[8] R. Cammack, *Nature* **1999**, *397*, 214 – 215.
[9] F. Gloaguen, T. B. Rauchfuss, *Chem. Soc. Rev.* **2009**, *38*, 100 – 108.
[10] C. Tard, C. J. Pickett, *Chem. Rev.* **2009**, *109*, 2245 – 2274.
[11] G. A. N. Felton, C. A. Mebi, B. J. Petro, A. K. Vannucci, D. H. Evans, R. S. Glass, D. L. Lichtenberger, *J. Organomet. Chem.* **2009**, *694*, 2681 – 2699.
[12] F. Wang, W.-G. Wang, H.-Y. Wang, G. Si, C.-H. Tung, L.-Z. Wu, *ACS Catal.* **2012**, *2*, 407 – 416.
[13] L. Wang, Z. Xiao, X. Ru, X. Liu, *RSC Adv.* **2011**, *1*, 1211 – 1219.
[14] S. Ibrahim, P. M. Woi, Y. Alias, C. J. Pickett, *Chem. Commun.* **2010**, *46*, 8189 – 8191.
[15] C. Zhan, X. Wang, Z. Wei, D. J. Evans, X. Ru, X. Zeng, X. Liu, *Dalton Trans.* **2010**, *39*, 11255 – 11262.
[16] M. L. Singleton, J. H. Reibenspies, M. Y. Darensbourg, *J. Am. Chem. Soc.* **2010**, *132*, 8870 – 8871.
[17] M. L. Singleton, D. J. Crouthers, R. P. Duttweiler III, J. H. Reibenspies, M. Y. Darensbourg, *Inorg. Chem.* **2011**, *50*, 5015 – 5026.
[18] M. K. Harb, U.-P. Apfel, J. Kübel, H. Görls, G. A. N. Felton, T. Sakamoto, D. H. Evans, R. S. Glass, D. L. Lichtenberger, M. Elkhateeb, W. Weigand, *Organometallics* **2009**, *28*, 6666 – 6675.
[19] M. K. Harb, U.-P. Apfel, J. Kübel, H. Görls, G. A. N. Felton, T. Sakamoto, D. H. Evans, R. S. Glass, D. L. Lichtenberger, M. Elkhateeb, W. Weigand, *Organometallics* **2010**, *29*, 5330 – 5340.
[20] W.-G. Wang, F. Wang, H.-Y. Wang, G. Si, C.-H. Tung, L.-Z. Wu, *Chem. Asian J.* **2010**, *5*, 1796 – 1803.
[21] A. P. S. Samuel, D. T. Co, C. L. Stern, M. R. Wasielewski, *J. Am. Chem. Soc.* **2010**, *132*, 8813 – 8815.
[22] W.-G. Wang, F. Wang, H.-Y. Wang, C.-H. Tung, L.-Z. Wu, *Dalton Trans.* **2012**, *41*, 2420 – 2426.
[23] H. Cui, M. Hu, H. Wen, G. Chai, C. Ma, H. Chen, C. Chen, *Dalton Trans.* **2012**, *41*, 13899 – 13907.
[24] H.-Y. Wang, G. Si, W.-N. Cao, W.-G. Wang, Z.-J. Li, F. Wang, C.-H. Tung, L.-Z. Wu, *Chem. Commun.* **2011**, *47*, 8406 – 8408.
[25] P. Poddutoori, D. T. Co, A. P. S. Samuel, C. H. Kim, M. T. Vagnini, M. R. Wasielewski, *Energy Environ. Sci.* **2011**, *4*, 2441 – 2450.
[26] Y. Na, M. Wang, J. Pan, P. Zhang, B. Åkermark, L. Sun, *Inorg. Chem.* **2008**, *47*, 2805 – 2810.
[27] D. Streich, Y. Astuti, M. Orlandi, L. Schwartz, R. Lomoth, L. Hammarström, S. Ott, *Chem. Eur. J.* **2010**, *16*, 60 – 63.
[28] P. Zhang, M. Wang, Y. Na, X. Li, Y. Jiang, L. Sun, *Dalton Trans.* **2010**, *39*, 1204 – 1206.
[29] F. Wang, W.-G. Wang, X.-J. Wang, H.-Y. Wang, C.-H. Tung, L.-Z. Wu, *Angew. Chem.* **2011**, *123*, 3251 – 3255; *Angew. Chem. Int. Ed.* **2011**, *50*, 3193 – 3197.
[30] W.-N. Cao, F. Wang, H.-Y. Wang, B. Chen, K. Feng, C.-H. Tung, L.-Z. Wu, *Chem. Commun.* **2012**, *48*, 8081 – 8083.
[31] Y. Sano, A. Onoda, T. Hayashi, *Chem. Commun.* **2011**, *47*, 8229 – 8231.
[32] A. Roy, C. Madden, G. Ghirlanda, *Chem. Commun.* **2012**, *48*, 9816 – 9818.
[33] X. Li, M. Wang, D. Zheng, K. Han, J. Dong, L. Sun, *Energy Environ. Sci.* **2012**, *5*, 8220 – 8224.
[34] X. Li, M. Wang, L. Chen, X. Wang, J. Dong, L. Sun, *ChemSusChem* **2012**, *5*, 913 – 919.
[35] A. M. Kluwer, R. Kapre, F. Hartl, M. Lutz, A. L. Spek, A. M. Brouwer, P. W. N. M. van Leeuwen, J. N. H. Reek, *Proc. Natl. Acad. Sci. USA* **2009**, *106*, 10460 – 10465.
[36] H.-Y. Wang, W.-G. Wang, G. Si, F. Wang, C.-H. Tung, L.-Z. Wu, *Langmuir* **2010**, *26*, 9766 – 9771.
[37] F. Wen, X. Wang, L. Huang, G. Ma, J. Yang, C. Li, *ChemSusChem* **2012**, *5*, 849 – 853.
[38] T. W. Woolerton, S. Sheard, Y. S. Chaudhary, F. A. Armstrong, *Energy Environ. Sci.* **2012**, *5*, 7470 – 7490.
[39] R. Lomoth, S. Ott, *Dalton Trans.* **2009**, 9952 – 9959.
[40] N. Agmon, *Chem. Phys. Lett.* **1995**, *244*, 456 – 462.
[41] D. Marx, M. E. Tuckerman, J. Hutter, M. Parrinello, *Nature* **1999**, *397*, 601 – 604.
[42] I. Tomatsu, A. Hashidzume, A. Harada, *J. Am. Chem. Soc.* **2006**, *128*, 2226 – 2227.
[43] M. Nakahata, Y. Takashima, H. Yamaguchi, A. Harada, *Nat. Commun.* **2011**, *2*, 511 – 516.
[44] Z. Shen, H. Duan, H. Frey, *Adv. Mater.* **2007**, *19*, 349 – 352.
[45] C. Zhai, H. Zhang, N. Du, B. Chen, H. Huang, Y. Wu, D. Yang, *Nanoscale Res. Lett.* **2011**, *6*, 31 – 35.
[46] D. R. Baker, P. V. Kamat, *Langmuir* **2010**, *26*, 11272 – 11276.
[47] H. Zhang, Z. Zhou, B. Yang, M. Gao, *J. Phys. Chem. B* **2003**, *107*, 8 – 13.
[48] J. C. Benegas, R. F. M. J. Cleven, M. A. G. T. van den Hoop, *Anal. Chim. Acta* **1998**, *369*, 109 – 114.
[49] S. J. Borg, T. Behrsing, S. P. Best, M. Razavet, X. Liu, C. J. Pickett, *J. Am. Chem. Soc.* **2004**, *126*, 16988 – 16999.
[50] D. Chong, I. P. Georgakaki, R. Mejia-Rodriguez, J. Sanabria-Chinchilla, M. P. Soriaga, M. Y. Darensbourg, *Dalton Trans.* **2003**, 4158 – 4163.
[51] R. Mejia-Rodriguez, D. Chong, J. H. Reibenspies, M. P. Soriaga, M. Y. Darensbourg, *J. Am. Chem. Soc.* **2004**, *126*, 12004 – 12014.
[52] F. Gloaguen, J. D. Lawrence, T. B. Rauchfuss, *J. Am. Chem. Soc.* **2001**, *123*, 9476 – 9477.
[53] A. B. Ellis, S. W. Kaiser, J. M. Bolts, M. S. Wrighton, *J. Am. Chem. Soc.* **1977**, *99*, 2839 – 2848.
[54] H. Davenport, C. Jeffreys, R. Warner, *J. Biol. Chem.* **1937**, *117*, 237 – 279.
[55] J. Aldana, Y. A. Wang, X. Peng, *J. Am. Chem. Soc.* **2001**, *123*, 8844 – 8850.

